CONTROL THE SURFACE CHEMISTRY OF CARBON NANODOTS BY ENGINEERING THE PRECURSOR ACID/AMINE RATIO

Pham Thi Thu Trang[1*], Tran Thi Khanh Linh[1], Bui Huy Hoang[2], Mai Xuan Dung[2], Tran Khanh Hoa[3], Vu Thi Phuong Anh[4], Nguyen Van Hao[4], Nguyen Thi Thanh[5]
[1]Vietnam Military Medical University, [2]Hanoi Pedagogical University 2,
[3]Thuy Loi University, [4]TNU - University of Sciences, [5]Vietnam National University of Agriculture

ARTICLE INFO

Received: 20/02/2025
Revised: 05/5/2025
Published: 05/5/2025

KEYWORDS

Carbon dots
Functional group
Surface chemistry
Hydrothermal
Energy levels

ABSTRACT

Controlling the surface functional groups of carbon nanodots is important to deploy carbon nanodots in various applications, such as visible-light photocatalysts, nanobiosensors, and multifunctional materials. In this study, we prepared a series of carbon nanodots by hydrothermal treatment mixtures of citric acid and ethylenediamine with different citric acid/ethylenediamine ratios. By using Fourier transform infrared, photoluminescent, and UV-Vis spectroscopies, it was demonstrated that the surface chemistry of carbon nanodot changed from carboxy-rich to amino-rich when the citric acid/ ethylenediamine ratio decreased. All carbon nanodots had a common absorption band at about 350 nm while their emission quantum yield varied from 2.5% to 63.0%. Theoretical calculations suggest that the energy levels of HOMO and LUMO of carboxy functionalized carbon nanodots were lower than those of amino-functionalized carbon nanodots while their bandgaps were similar. These research results provide important information for designing carbon nanodots for targeted applications.

ĐIỀU CHỈNH BỀ MẶT HÓA HỌC CỦA HẠT NANO CARBON BẰNG CÁCH THAY ĐỔI TỶ LỆ TIỀN CHẤT ACID/AMINE

Phạm Thị Thu Trang[1*], Trần Thị Khánh Linh[1], Bùi Huy Hoàng[2], Mai Xuân Dũng[2], Trần Khánh Hòa[3], Vũ Thị Phương Anh[4], Nguyễn Văn Hảo[4], Nguyễn Thị Thanh[5]
[1]Học viên Quân Y, [2]Trường Đại học Sư phạm Hà Nội 2, [3]Trường Đại học Thủy lợi
[4]Trường Đại học Khoa học - ĐH Thái Nguyên, [5]Học viện Nông nghiệp Việt Nam

THÔNG TIN BÀI BÁO

Ngày nhận bài: 20/02/2025
Ngày hoàn thiện: 05/5/2025
Ngày đăng: 05/5/2025

TỪ KHÓA

Hạt carbon
Nhóm chức
Hóa học bề mặt
Thủy nhiệt
Mức năng lượng

TÓM TẮT

Điều chỉnh bề mặt hóa học của hạt nano carbon có ý nghĩa quan trọng để triển khai ứng dụng của hạt nano carbon trong một số lĩnh vực khác nhau như xúc tác quang hóa, y sinh và chế tạo vật liệu đa chức. Trong nghiên cứu này, chúng tôi tổng hợp các mẫu hạt nano carbon bằng cách thủy nhiệt hỗn hợp axit citric và ethylenediamine khác nhau về tỷ lệ axit citric/ethylenediamine. Nghiên cứu hạt nano carbon bằng phổ hồng ngoại, phổ huỳnh quang và phổ hấp thụ UV-Vis, chúng tôi nhận thấy bề mặt của hạt nano carbon thay đổi từ giàu carboxy sang giàu amino khi giảm tỷ lệ axit citric/ethylenediamine. Các hạt nano carbon đều có chung một đỉnh hấp thụ ở khoảng 350 nm trong khi hiệu suất phát xạ lượng tử thay đổi trong khoảng từ 2,5% đến 63,0%. Tính toán lý thuyết cho thấy vị trí năng lượng của HOMO và LUMO của hạt nano carbon chức năng hóa bởi carboxy thấp hơn so với hạt nano carbon chức năng hóa bằng amino trong khi độ rộng vùng cấm của chúng là tương tự nhau. Kết quả trình bày trong bài báo này cung cấp thông tin quan trọng để thiết kế hạt nano carbon phù hợp cho ứng dụng cụ thể.

DOI: https://doi.org/10.34238/tnu-jst.12097

* Corresponding author. *Email: ptttrang82@gmail.com*

1. Introduction

Carbon nanodots (CNDs) are nano-sized, carbon-based materials whose structure involves π-conjugated domains and surface functional groups [1]. CNDs could be synthesized either by cutting down macrostructures of carbon, e.g. carbon nanotubes and graphite or by fusing molecular precursors into nano-sized carbon structures. However, CNDs are more preferably synthesized by bottom-up approaches, such as hydrothermal or solvothermal methods because they allow to use of a great number of carbon precursors [2]–[5]. CNDs synthesized by bottom-up procedures usually contain molecular-like fluorophore that, in addition to the conjugated component, greatly influences the absorption and emission properties of CNDs [6], [7]. Because of the covalent bonding nature in a CND, the surface functional groups also affect the optical properties of CNDs by increasing or decreasing the confinement space originated by conjugated components [8]–[10]. Additionally, surface functional groups modify the energy levels of HOMO (the highest occupied molecular orbital) and LUMO (the lowest unoccupied molecular orbital) that are important to design visible photocatalyst [9], [10]. Furthermore, surface functional groups determine the solubility of CNDs [3], influence the interactions between CNDs and the dispersing environment [11], [12], and govern the interactions between CNDs and an analyte in sensing applications [2], [4], [13]–[15]. Therefore, control of the surface functional groups of CNDs is of importance to consider their potential applications. Post-surface modifications based on carbon chemistry that usually involve multiple steps could be used to change the surface of CNDs [16]. Alternative methods that are simple and allow the synthesis of CNDs to have targeted functional groups are strongly demanded. Herein, we synthesized a series of CNDs using mixtures of citric acid (CA) and ethylenediamine (EDA), which are widely used precursors in the synthesis of blue-emitting CNDs [7], [17] to correlate the changes in the surfaces of CNDs and the CA/EDA ratio. It has been demonstrated that the surface functional groups of CNDs could be controlled as carboxy (-COOH) or amino (-NH_2) by changing the initial CA/EDA ratio. Carboxy-functionalized CNDs (denoted as CND-COOH) could have an emission quantum yield (QY) as high as 34.0% while that of amino-functionalized (CND-NH_2) was 63.0%.

2. Experimental section

2.1. Chemicals and equipments

Chemicals including citric acid monohydrate (99.5%) and ethylenediamine (99.5%) were purchased from Aladdin Chemicals and used without any purifications. Double-distilled water was freshly prepared in the laboratory and used as a synthetic solvent. A 50 mL, polypropiolactone (PPL) lined autoclave was used as a hydrothermal reactor. A Binder ED115 electric oven was used to control the synthetic temperature.

2.2. The synthesis and purification of CNDs

To a PPL vessel, 5M CA and EDA aqueous solutions were added, mixed, and aerated with nitrogen gas before being transferred into an autoclave reactor. The reactor was placed in an electric oven at 200 ^oC for 4 hours to conduct the hydrothermal synthesis. After being cooled to room temperature, the resultant mixture was dialyzed against water for 48 hours using a dialysis bag having a molecular cutoff of 2000 Dalton. The CND solutions in the dialysis bag were then filtered through PTFE 0.22 μ syringe filters to remove large particles. Finally, the resultant CND solutions were rotary evaporated to obtain dried solid CNDs which were stored at 4 ^oC till being used.

2.3. Characterizations

The absorption spectra of CNDs dissolved in water were measured using a Shimadzu UV-2450 spectrometer. Photoluminescence (PL) and photoexcitation (PLE) spectra of CND solutions were recorded on a FLS1000 spectrometer. A Jasco FT/IR6300 spectrometer was used to conduct Fourier-

transform infrared (FT-IR) spectra of CNDs by a KBr method. Transmission electron microscope (TEM) images of CNDs were taken on a JEM 2100 microscope operating at 200 kV using LaB6 filament. A D8 Advanced X-ray diffractometer was used to measure the X-ray diffraction pattern of dried CNDs. To determine the QY of CNDs, a solution of quinine sulfate dissolved in H_2SO_4 0.5M was used as a standard solution. The standard solution and CND solutions were prepared so that the absorbance at 350 nm was about 0.1. Their PL spectra were measured using the same conditions when excited at 350 nm. QY of CNDs was calculated using equation (1), where I_R and I_{CND} are the PL intensity of the standard and CND solution; A_R and A_{CND} are the absorbance of the standard and CND solution at 350 nm; and Q_R of 54% is the QY of quinine sulfate.

$$QY_{CND} = Q_R \frac{I_{CND}}{I_R} \frac{A_R}{A_{CND}} \quad (1)$$

Theoretical calculations were performed in gass phase using DFT method and B3LYP/6-31g basic set available in GO09. The energy levels of HOMO and LUMO of optimized structures were extracted by GaussView 5.0.8 program.

3. Results and discussion

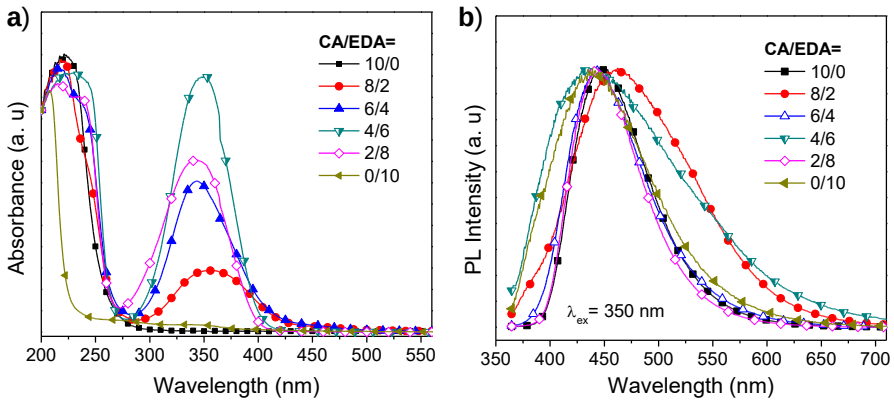

Figure 1. *a) The UV-Vis absorption and b) normalized PL spectra of CNDs*

The absorption spectra of CNDs with varying CA/EDA ratiod are shown in Figure 1a. It revealed that when both CA and EDA were used, the resultant CNDs had a common absorption band at about 350 nm. This characteristic absorption peak was attributed to the existence of 5-oxo-1,2,3, 5-tetrahydroimidazo[1,2-a]pyridine-7-carboxylic acid (IPCA) fluorophore within the CNDs [18]–[20]. The existence of ICPA could be briefly explained as follows: CA and EDA react to form amides that partially undergo intermolecular condensation to form IPCA [21]. Under hydrothermal conditions, continuous condensation and carbonization involved amides, IPCA, and other oligomers forming π-conjugated molecules. IPCA and those conjugated molecules assembled into CNDs induced by π-π attraction [22], [23]. When excited at 350 nm, the PL spectra of CNDs shown in Figure 1b were broad, ranging from 375 nm to 625 nm. The PL maximum position varied from 438 nm to 460 nm depending on the CA/EDA ratio but no tendency was observed. It is noted that CNDs with CA/EDA of 10/0 or of 0/10 also had similar PL spectra to other CNDs although they did not involve IPCA in their structure as indicated by the absence of IPCA absorption peak at 350 nm (Figure 1a). It was because the emission regions originated from ICPA, mixtures of π-conjugated components, and carbogenous structures were similar [16], [24], [25].

The surface chemistry of CDNs was studied by FT-IR and the results are shown in Figure 2. All CNDs had a broad absorption band in the long-wavelength region (3200-3600 cm^{-1}) indicating that CNDs had polar bonds, such as O–H (3600 cm^{-1}) and N–H (3450 cm^{-1}) bonds. As the CA/EDA ratio increased from 10/0 to 0/10, the IR feature of CNDs changed gradually from

EDA alone CND to CA alone CND. It is reasonable to assume EDA alone CND to be CND-NH_2 and CA alone CND to be CND-COOH. Three absorption features at 1650, 1710, and 1780 cm^{-1} were attributed to the stretching vibrations of C=O bonds in amide, carboxyl, and conjugated acid, respectively [20]. The absorption at 1780 cm^{-1} was only observed in CA/EDA= 10/0 sample while the absorption of C=O in –COOH groups was not observed in CNDs with CA/EDA ratios of less than 4/6. As the same time, the absorption of O–H bending at about 1205 cm^{-1} dissapeared as CA/EDA decreased to less than 4/6. Therefore, we can conclude that when the CA/EDA ratio is greater than 4/6 the surface of CNDs involves –COOH groups. Additionally, IR features of CA/EDA=2/8 and EDA alone samples were similar indicating that $–NH_2$ is the dominant functional group on the surface of CNDs.

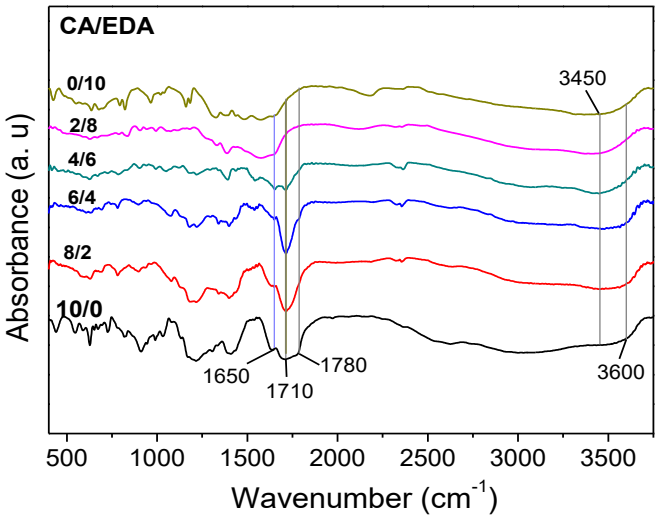

Figure 2. *FT-IR spectra of CNDs obtained at different CA/EDA ratios*

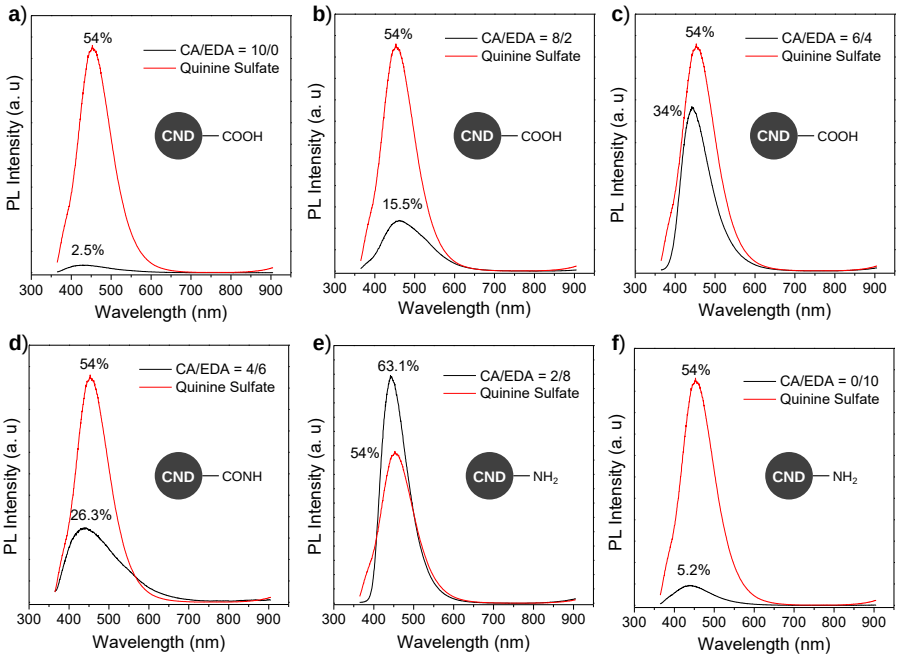

Figure 3. *PL spectra of CNDs in comparison with quinine sulfate when excited at 350 nm The CA/EDA ration was: a) 10/0, b) 8/2, c) 6/4, d) 4/6, e) 2/8, and f) 0/10*

In addition to the emission region, the emission quantum yield is an important factor of CNDs in many applications, such as bioimaging, light-converting materials, and light encryption. QY of CNDs with different CA/EDA ratios was determined by comparing with quinine sulfate whose QY is 54.0%. The results are shown in Figure 3. The QY varied from 2.5% to 63.0% depending on the CA/EDA ratio although the dependence was not in a clear trend. Those QY values were comparable to values reported by other groups [20]. Carboxy-functionalized CNDs that have the highest QY (34.0%) were obtained when the CA/EDA ratio was 6/4. If the CA/EDA ratio was 2/8 CND-NH_2 had the best QY of 63.0%.

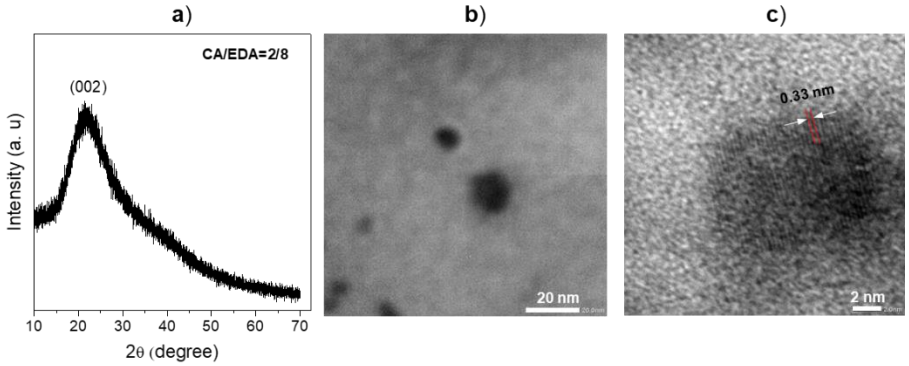

Figure 4. *a) X-ray diffraction pattern, b) TEM image, and c) HR-TEM image of CND-NH_2*

Because CND-NH_2 had the highest QY among CNDs, we studied further on the structure of CND-NH_2 by X-ray diffraction (XRD) and transmission electron microscope; the results are shown in Figure 4. XRD pattern of CND-NH_2 in Figure 4a exhibited a broad peak at 2 theta of 23^o which could be attributed to the diffraction from (002) plans of graphite structure [26], [27]. TEM image in Figure 4b shows individual CNDs as black dots whose diameter was in the 5.5-11.0 nm range. High-resolution TEM (HR-TEM) image in Figure 4c clearly shows a lattice feature with a d-spacing of 0.33 nm corresponding to $d_{(002)}$ of the graphitic carbon.

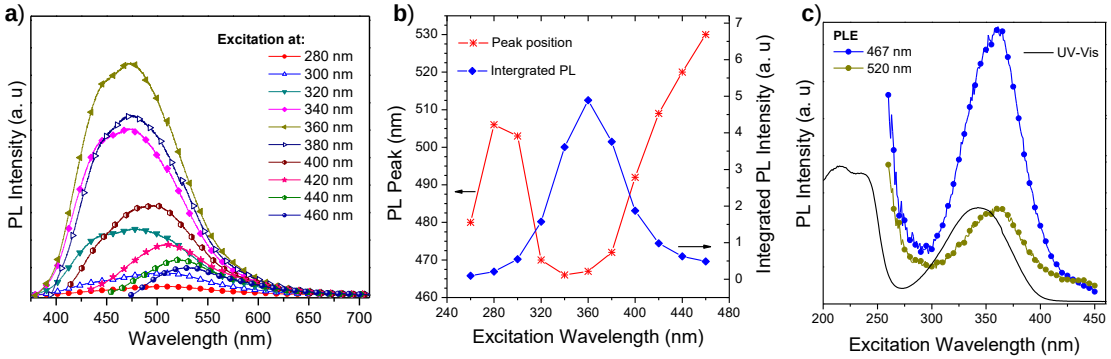

Figure 5. *Optical characteristics of CND-NH_2: a) Excitation-dependent PL spectra, b) Effect of the excitation wavelength on the PL position and PL intensity, and* ***c)*** *PLE and absorption spectra*

We studied the optical properties of CND-NH_2 in detail and the results are summarized in Figure 5. PL spectrum of CNDs depended on the excitation wavelength (Figure 5a). Concretely, the emission intensity reached maximum value when the excitation wavelengths were about 360 nm (Figure 5b). At the same time, the position of PL maximum was lowest, at about 467 nm, when CNDs were excited around 360 nm. When CNDs were excited above 360 nm, the position of PL maximum increased gradually with the excitation wavelength. PLE observed at 467 nm and 520 nm exhibited a common band centered at 360 nm, which was similar to the absorption band (Figure 5c). To explain the optical properties of CNDs shown in Figure 5, we put a tentative mechanism in Figure 6. A CND involves IPCA fluorophore and conjugated domains assembled

in a carbogenic core whose surface is functionalized with -NH_2 groups, as in the case of CA/EDA of 2/8 (Figure 6ª). The absorption at 360 nm and the emission maximized at 467 nm likely originates from the IPCA component of CNDs. When the excitation was around 360 nm (upward arrow 1 in Figure 6b), the light was mostly absorbed by IPCA giving rise to IPCA emission at 467 nm (downward, blue arrow in Figure 6b). Photogenerated charges at ICPA could partially transfer to carbogenic component (noted by dashed arrows in Figure 6b) at which they recombine to emit light at the higher wavelength region, e.g. 520 nm (downward, green arrow in Figure 6b) as indicated by the PLE peak at 360 nm shown in Figure 5c. When CNDs were exposed to light above 360 nm, the carbogenic component was excited (upward arrow 2 in Figure 6b) and gave PL emission whose position increased with the excitation wavelength. Figure 5b shows that the emission from the carbogenic component was very inefficient when compared with the emission from the IPCA component. Shortly, ICPA fluorophore in CNDs dominates the absorption and emission properties of CNDs.

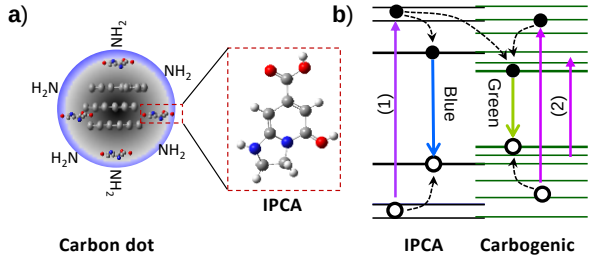

Figure 6. *Tentative structure: a) and optical mechanism b) of CND*

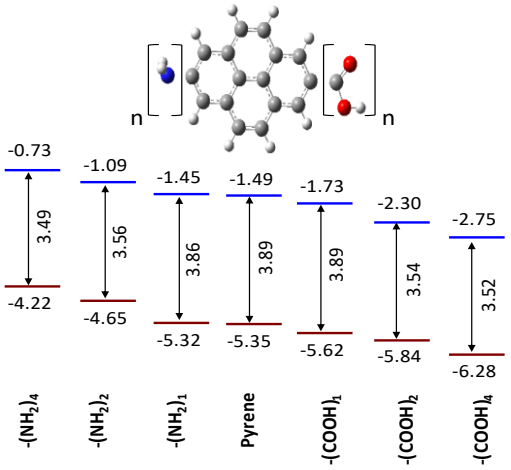

Figure 7. *Effects of surface functional groups on the electronic structure of CNDs*

Finally, to evaluate the fate of surface functional groups on the electronic properties of CNDs, we conducted DFT calculations on a simple model in which *n* groups of either -NH_2 or -COOH are bonded to a pyrene conjugated system. Energy levels (versus the vacuum level) of LUMO (blue lines) and HOMO (red lines) and energy gap of modeled CNDs with different functional groups are shown in Figure 7. Two tendencies are clearly revealed, including 1) as the number of functional groups increases the energy gap decreases and 2) the energy levels of CND-NH_2 are higher than those of CND-COOH. In photocatalyst applications, excited electron and hole occupy HOMO and LUMO, respectively. At those levels, electron and hole initiate redox reactions. Results in Figure 7 indicate that excited CND-NH_2 would have a higher reduction ability compared to CND-COOH counterpart. Those theoretical calculations are an important guideline for constructing CNDs for photocatalysts.

4. Conclusion

A series of carbon nanodots was successfully synthesized by hydrothermal treatment of CA-EDA mixtures with different CA/EDA ratios to study the effects of precursor ratio on the surface chemistry and the optical properties of obtained CNDs. Carboxy was the main functional group on the surface of CNDs when the CA/EDA ratio was greater than 4/6 while amino-functionalized CNDs were obtained when the CA/ED ratio was less than 2/8. The absorption and photoluminescent properties of CNDs were greatly affected by IPCA fluorophore. CNDs that had the highest emission quantum yield of 63.0% were CND-NH_2.

Theoretical calculations indicate that CND-NH_2 has higher HOMO and LUMO levels than CND-COOH while their energy gaps are similar. These research results could be used to design suitable carbon nanodots for diverse applications.

REFERENCES

[1] S. Zhu, Y. Song, X. Zhao, J. Shao, J. Zhang, and B. Yang, "The photoluminescence mechanism in carbon dots (graphene quantum dots, carbon nanodots, and polymer dots): current state and future perspective," *Nano Res.*, vol. 8, no. 2, pp. 355–381, Feb. 2015, doi: 10.1007/s12274-014-0644-3.

[2] T. D. Nguyen *et al.*, "Decorating conjugated fluorophore to PEI for photoluminescence sensing and interfacial electrolyte applications," *Mater. Lett.*, vol. 377, Aug. 2024, Art. no. 137444, doi: 10.1016/j.matlet.2024.137444.

[3] T. T.-H. Do *et al.*, "Control the solubility of carbon quantum dots by solvent engineering," *HPU2 J. Sci. Nat. Sci. Technol.*, vol. 2, no. 3, pp. 51–58, Dec. 2023, doi: 10.56764/hpu2.jos.2023.2.3.51-58.

[4] X.-D. Mai *et al.*, "One-pot synthesis of homogeneous carbon quantum dots/aluminum hydroxide composite and its application in Cu(II) detection," *Carbon Lett.*, vol. 34, pp. 603–609, Jan. 2024, doi: 10.1007/s42823-023-00676-z.

[5] T. Q. Nguyen *et al.*, "Universal method for preparation of metal-doped Carbon quantum dots," *TNU J. Sci. Technol.*, vol. 200, no. 07, pp. 3–9, 2019.

[6] D.-K. Nguyen, T.-S. Le, Q.-T. Le, and X.-D. Mai, "The roles of intermediate fluorophores on the optical properties of bottom-up synthesized carbon nanodots," *HPU2 J. Sci. Nat. Sci. Technol.*, vol. 2, no. 2, pp. 68–82, 2023, doi: 10.56764/hpu2.jos.2023.2.2.68-82.

[7] X.-D. Mai, T. T. K. Chi, T.-C. Nguyen, and V.-T. Ta, "Scalable synthesis of highly photoluminescence carbon quantum dots," *Mater. Lett.*, vol. 268, Jun. 2020, Art. no. 127595, doi: 10.1016/j.matlet.2020.127595.

[8] S. Zhu *et al.*, "Photoluminescence mechanism in graphene quantum dots: Quantum confinement effect and surface/edge state," *Nano Today*, vol. 13, pp. 10–14, 2017, doi: 10.1016/j.nantod.2016.12.006.

[9] H. Li *et al.*, "Water-soluble fluorescent carbon quantum dots and photocatalyst design," *Angew. Chemie - Int. Ed.*, vol. 49, no. 26, pp. 4430–4434, 2010, doi: 10.1002/anie.200906154.

[10] S. H. Jin, D. H. Kim, G. H. Jun, S. H. Hong, and S. Jeon, "Tuning the photoluminescence of graphene quantum dots through the charge transfer effect of functional groups," *ACS Nano*, vol. 7, no. 2, pp. 1239–1245, 2013, doi: 10.1021/nn304675g.

[11] Q.-B. Hoang, V.-T. Mai, D.-K. Nguyen, D. Q. Truong, and X.-D. Mai, "Crosslinking induced photoluminescence quenching in polyvinyl alcohol-carbon quantum dot composite," *Mater. Today Chem.*, vol. 12, pp. 166–172, Jun. 2019, doi: 10.1016/j.mtchem.2019.01.003.

[12] X. Xu *et al.*, "Surface functional carbon dots: Chemical engineering applications beyond optical properties," *J. Mater. Chem. C*, vol. 8, no. 46, pp. 16282–16294, 2020, doi: 10.1039/d0tc03805a.

[13] X.-D. Mai *et al.*, "Homogeneous and highly photoluminescent composites based on in-situ formed fluorophores in PVA blends," *Mater. Lett.*, vol. 319, Jul. 2022, Art. no. 132269, doi: 10.1016/j.matlet.2022.132269.

[14] X.-D. Mai *et al.*, "The synthesis of polymeric nano carbon from foods and the application in Pb(II) detection," *TNU J. Sci. Technol.*, vol. 189, no. 13, pp. 45–51, 2018.

[15] H. Shabbir, E. Csapó, and M. Wojnicki, "Carbon quantum dots: The role of surface functional groups and proposed mechanisms for metal ion sensing," *Inorganics*, vol. 11, no. 6, 2023, doi: 10.3390/inorganics11060262.

[16] T.-H. T. Dang, V.-T. Mai, Q.-T. Le, N.-H. Duong, and X.-D. Mai, "Post-decorated surface fluorophores enhance the photoluminescence of carbon quantum dots," *Chem. Phys.*, vol. 527, Nov. 2019, Art. no. 110503, doi: 10.1016/j.chemphys.2019.110503.

[17] Q. Fang *et al.*, "Luminescence origin of carbon based dots obtained from citric acid and amino group-containing molecules," *Carbon*, vol. 118, pp. 319–326, 2017, doi: 10.1016/j.carbon.2017.03.061.

[18] Y. Song *et al.*, "Investigation from chemical structure to photoluminescent mechanism: A type of carbon dots from the pyrolysis of citric acid and an amine," *J. Mater. Chem. C*, vol. 3, no. 23, pp. 5976–5984, 2015, doi: 10.1039/c5tc00813a.

[19] X.-D. Mai *et al.*, "The thermal preparation of luminescent pmma composite using citric acid and ethylenediamine," *TNU J. Sci. Technol.*, vol. 227, no. 16, pp. 62–67, Oct. 2022, doi: 10.34238/tnu-jst.6470.

[20] A. M. Vervald, K. A. Laptinskiy, M. Y. Khmeleva, and T. A. Dolenko, "Toward carbon dots from citric acid and ethylenediamine, part 1: Structure, optical properties, main luminophore at different stages of synthesis," *Carbon Trends*, vol. 19, 2025, Art. no. 100452, doi: 10.1016/j.cartre.2025.100452.

[21] M. Pykal *et al.*, "Thermodynamics and kinetics of early stages of carbon dot formation: A case of citric acid and ethylenediamine reaction," *Nanoscale*, vol. 17, pp. 7780-7789, 2025, doi: 10.1039/d4nr04420g.

[22] M. Otyepka, M. Langer, M. Paloncýová, and M. Medved', "Molecular fluorophores self-organize into c-dot seeds and incorporate into c-dot structures," *J. Phys. Chem. Lett.*, vol. 11, no. 19, pp. 8252–8258, 2020, doi: 10.1021/acs.jpclett.0c01873.

[23] P. Duan, B. Zhi, L. Coburn, C. L. Haynes, and K. Schmidt-Rohr, "A molecular fluorophore in citric acid/ethylenediamine carbon dots identified and quantified by multinuclear solid-state nuclear magnetic resonance," *Magn. Reson. Chem.*, vol. 58, no. 11, pp. 1130–1138, 2020, doi: 10.1002/mrc.4985.

[24] M. Shamsipur, A. Barati, A. A. Taherpour, and M. Jamshidi, "Resolving the multiple emission centers in carbon dots: From fluorophore molecular states to aromatic domain states and carbon-core states," *J. Phys. Chem. Lett*., vol. 9, no. 15, pp. 4189–4198, 2018, doi: 10.1021/acs.jpclett.8b02043.

[25] M. Fu *et al*., "Carbon dots: A unique fluorescent cocktail of polycyclic aromatic hydrocarbons," *Nano Lett*., vol. 15, no. 9, pp. 6030–6035, 2015, doi: 10.1021/acs.nanolett.5b02215.

[26] X. Mai, Y. T. H. Phan, and V. Nguyen, "Excitation-independent emission of carbon quantum dot solids," *Adv. Mater. Sci. Eng*., vol. 2020, pp. 1–5, Dec. 2020, doi: 10.1155/2020/9643168.

[27] V. T. Mai, T. P. Le, A. D. Vu, X. B. Nguyen, and X. D. Mai, "Enhanced energy transfer in carbon quantum dot solids," *TNU J. Sci. Technol*., vol. 225, no. 06, pp. 419–423, 2020.